



HAL
open science

Revisiting the methods of determining hydraulic conductivity of saturated expansive clays in low-compressibility zone

Wei Su, Yu-Jun Cui, Feng Zhang, Weimin Ye

► **To cite this version:**

Wei Su, Yu-Jun Cui, Feng Zhang, Weimin Ye. Revisiting the methods of determining hydraulic conductivity of saturated expansive clays in low-compressibility zone. *Journal of Rock Mechanics and Geotechnical Engineering*, 2020, 12 (5), pp.1131-1136. 10.1016/j.jrmge.2020.01.004 . hal-03045843

HAL Id: hal-03045843

<https://enpc.hal.science/hal-03045843>

Submitted on 17 Oct 2022

HAL is a multi-disciplinary open access archive for the deposit and dissemination of scientific research documents, whether they are published or not. The documents may come from teaching and research institutions in France or abroad, or from public or private research centers.

L'archive ouverte pluridisciplinaire **HAL**, est destinée au dépôt et à la diffusion de documents scientifiques de niveau recherche, publiés ou non, émanant des établissements d'enseignement et de recherche français ou étrangers, des laboratoires publics ou privés.



Distributed under a Creative Commons Attribution - NonCommercial 4.0 International License

Abstract

The hydraulic conductivity of saturated clays is commonly determined either directly by monitoring water flux or indirectly based on Terzaghi's consolidation equation. Similar results are often obtained from the two methods; but sometimes there is significant difference between the two, in particular for expansive soils. In this study, the hydraulic conductivities determined by the two methods are first compared based on existing data in the literature. The indirect method is then revisited attempting to explain the difference identified. A modified effective stress, considering physic-chemical interaction between face-to-face oriented particles, is finally introduced to better describe the compressibility of expansive clays and to further improve the indirect method in determining hydraulic conductivity of such soils in the low-compressibility zone. Extra tests were performed on Gaomiaozi (GMZ) bentonite slurry and the results obtained allowed the modified indirect method to be verified.

Keywords: expansive clays; laboratory tests; hydraulic conductivity; Terzaghi's consolidation equation; modified effective stress

Notation

c_v : consolidation coefficient

m_v : coefficient of compressibility

m_v' : modified coefficient of compressibility

γ_w : unit weight of water

e : void ratio

σ' : effective stress

σ_v : vertical total stress

σ_v' : vertical effective stress

σ_s : mineral to mineral contact stress

R : total interparticle repulsion divided by total interparticle area

A : total interparticle attraction divided by total interparticle area

σ : average net repulsive force acting on the bound water-film area divided by the total cross-sectional area

σ^{R-A} : net stress acting on water-films between clay particles

P_s : swelling pressure

k : hydraulic conductivity

k_d, k_{ind} : hydraulic conductivity determined directly and indirectly

k_{ind}' : hydraulic conductivity calculated using modified effective stress

1 **Introduction**

2 The hydraulic conductivity k is one of the key parameters in geotechnical and geo-
3 environmental engineering. Many efforts have been devoted to the measurement of this
4 parameter in both field and laboratory conditions. In the laboratory, the hydraulic conductivity
5 is commonly determined either directly by monitoring water flux or indirectly based on
6 Terzaghi's consolidation equation. Tavenas et al. (1983) compared the direct and indirect
7 measurement methods for natural clays and observed that the indirect method overestimated
8 the values at relatively large void ratios while underestimated the values at smaller void ratios.
9 The authors attributed the difference to the adopted assumptions of constant k , compressibility
10 and coefficient of consolidation during each consolidation stage, as well as the ways of
11 interpreting the consolidation-time curves on the basis of Terzaghi's consolidation theory.
12 Mesri et al. (1994) reported that the indirect method typically underestimates the value of
13 permeability by a factor of 2. Therefore, in the estimation of the settlement of Kansai
14 International Airport Islands, the values of hydraulic conductivity of the involved Holocene
15 marine clay determined by the indirect method were multiplied by 2 (Mesri and Funk, 2015).

16
17 This paper aims at better clarifying the indirect method of determining the hydraulic
18 conductivity of expansive clays. First, reported k data for remoulded, undisturbed and
19 compacted clayey soils, determined directly and indirectly in one-dimensional condition were
20 collected. Then, the parameters used for indirectly determining k were analysed one by one in
21 order to better understand the difference between the direct and the indirect methods. Thereby,
22 the significance of physico-chemical effects between the bound water around clay particles in
23 controlling the response of dense clay to external loading was identified. A modified effective
24 stress concept based on this was postulated and introduced in the Terzaghi's consolidation
25 theory, aiming to narrow the difference between the direct and the indirect methods. Finally,
26 the modified method was verified based on existing data from the literature and complementary

27 data from tests on GMZ bentonite. This study suggests the necessity of introducing the modified
28 effective stress concept into the Terzaghi's consolidation theory for active expansive clays in
29 the low-compressibility zone.

30 **Direct and indirect methods for k determination**

31 Generally, in a conventional step-loading oedometer test, k can be indirectly calculated at each
32 loading step based on Terzaghi's consolidation theory as follows:

$$33 \quad k = c_v m_v \gamma_w \quad (1)$$

34 where, k is the hydraulic conductivity (m/s), c_v is the consolidation coefficient (m^2/s), m_v is the
35 coefficient of compressibility (kPa^{-1}), γ_w is the unit weight of water (taken equal to 10 kN/m^3 in
36 this study).

37

38 Parameter c_v reflects the rate at which a saturated clay undergoes consolidation when subjected
39 to an incremental load. In practice, the methods proposed by Casagrande and Fadum (1944)
40 and Taylor (1948) are routinely used to estimate the c_v from the settlement-time curve at each
41 loading step. It appears that this parameter shows mineral-dependence and varies with the stress
42 state of soil (Retnamony et al., 1998; Sridharan and Nagaraj, 2004).

43

44 At the end of a loading step i , with corresponding void ratio e , m_v can be determined as follows:

$$45 \quad m_{v,i} = \frac{\Delta e_i}{\Delta \sigma'_{v,i} (1 + e_{i-1})} \quad (2)$$

46 Obviously, any factors involved in the determination of soil deformation and vertical effective
47 stress increment $\Delta \sigma'_v$ can influence the value of m_v .

48

49 Meanwhile, at the end of each consolidation stage, the hydraulic conductivity k can be
50 determined directly based on Darcy's law by connecting the base of the soil specimen to a
51 burette using falling head method or to a pressure/volume controller using constant head
52 method (ASTM D5856; ASTM D7100).

53 Comparison of the two methods based on the literature data

54 In this section, the direct and indirect results reported in the literature are collected and
55 compared. The sources of data are summarized in Table 1. The reliability of indirect k values
56 is evaluated by the ratio k_d/k_{ind} , where k_d and k_{ind} are the direct and indirect hydraulic
57 conductivities, respectively. The k_d/k_{ind} results in the high-compressibility zone are plotted in
58 Fig. 1, together with the $e-\lg\sigma'_v$ curves. It is observed that the values of k_d/k_{ind} exhibit a large
59 scatter. However, most of them are close to unity (mostly from 0.5 to 1.1). This suggests that
60 at this stage, the indirect method is reasonably valid. Nevertheless, in the case where very high
61 stress is applied and the soil compressibility changed to very small value, k_d/k_{ind} turns to be
62 much larger than unity (Fig. 1b,c), suggesting that the indirect method becomes less valid.
63 Further examination of Eq. 1 shows that the reliability of indirect value k mainly depends on
64 the accuracy of c_v and m_v . As pointed out by Tavenas et al. (1979), clays in the normally
65 consolidated state exhibit significant variations in terms of c_v and m_v with changes in void ratio.
66 This is confirmed by the results of three bentonite specimens shown in Fig. 2 and Fig. 3: a
67 decreasing trend is identified for c_v (Fig. 2) and m_v (Fig. 3). Tavenas et al. (1983) also reported
68 that the reduction of c_v near the drainage boundary is much faster than in other part of specimen.
69 Obviously, this finding is contradictory to the assumption of constant c_v at each loading step.
70 Thereby, the indirect value k is affected by this assumption, explaining the fluctuation observed
71 in Fig. 1a.

72

73 As the consolidation process steps into the low-compressibility zone, small strain is recorded
74 and the variations in c_v and m_v become moderate (Figs. 2 and 3). These observations are more
75 consistent with the Terzaghi's assumptions, theoretically making this theory more applicable
76 in this zone. However, it is observed that k_d/k_{ind} starts to be larger than unity (see Fig. 1b,c). It
77 is commonly admitted that in this zone all macro-pores have collapsed and further loading gives
78 rise to compression of well orientated face-to-face particles. In such orientated microstructure,

79 the physic-chemical interaction between clay particles and absorbed water is enhanced and
80 starts to govern the global volume change behaviour of specimen (Cui et al., 2013). Mesri and
81 Olson (1971) also pointed out that while investigating the hydraulic conductivity of soils, it is
82 important to consider not only the mechanical variables (mainly the size, shape and geometrical
83 arrangement of the clay particles), but the physico-chemical variables (surface charge density
84 and distribution, valence of the adsorbed cations as well as the properties of the involved fluid).
85 From this point of view, the stress induced by the physico-chemical interactions should be
86 accounted for when calculating the effective stress, which could impact the determination of m_v ,
87 by Eq. 2.

88

89 **Introduction of a modified effective stress in the indirect method**

90 For saturated soils subjected to an external loading, Terzaghi (1936) introduced an effective
91 stress in form of Eq.3 and stated that mechanical responds, such as compression, distortion and
92 changes in shearing resistance, etc., are exclusively due to changes in effective stress:

$$93 \quad \sigma' = \sigma_t - u_w \quad (3)$$

94 where σ' is the effective stress ($\text{ML}^{-1}\text{T}^{-2}$), σ_t is the total external stress ($\text{ML}^{-1}\text{T}^{-2}$) and u_w is the
95 pressure ($\text{ML}^{-1}\text{T}^{-2}$) of the free bulk water.

96

97 However, for expansive clayey soils, in addition to free pore water, there are another two kinds
98 of water: 1) crystalline water which is strongly adsorbed and attached to clay sheets; 2) double
99 layer water which is well adsorbed to clay particles. Under mechanical loading, free pore water
100 was compressed, generating pore water pressure. The dissipation of such pressure leads to the
101 volume change of soil and this process is commonly known as soil consolidation. However, for
102 the adsorbed water, the changes of its pressure is controlled by the physico-chemical
103 interactions between the bound water around clay particles and this pressure is interparticle
104 distance-independent.

105

106 Depending on the circumstances, these two kinds of water pressure could act separately or
107 together to control the volumetric behaviour of clayey soils. In a consolidating clay with high
108 compressibility, a large number of large pores exist and the drainage of “free” water in the large
109 pores is responsible for the volume change. This is accompanied by the development of
110 particles reorientation and thus the progressive enhancement of physico-chemical interactions
111 between bound water and clay particles (Bolt, 1956; Mašín and Khalili, 2015); as the
112 consolidation keeps proceeding in the low compressibility zone, the large pores disappear as all
113 clay particles are normally well orientated, the “free” water is thoroughly drained out and all
114 water can be considered as adsorbed water. Thus, the common pore water pressure can be taken
115 equal to zero and the physico-chemical effects will control the response of the dense clay to
116 applied loading. However, water can still flow under very high gradients (Pusch et al., 1987).
117 In such case, the physico-chemical stress can be taken equal to the swelling pressure (Zhang,
118 2017).

119
120 Sridharan and Rao (1973) suggested accounting the electrical forces acting in the water-films
121 around clay particles into the common Terzaghi’s effective stress equation. Lambe (1960)
122 included the electrical attractive and repulsive forces between water-films around clay particles
123 as follows:

$$124 \quad \sigma' = \sigma_s + R - A \quad (4)$$

125 where σ_s is the mineral to mineral contact stress ($\text{ML}^{-1}\text{T}^{-2}$), R is the total interparticle repulsion
126 divided by total interparticle area ($\text{ML}^{-1}\text{T}^{-2}$), A is the total interparticle attraction divided by
127 total interparticle area ($\text{ML}^{-1}\text{T}^{-2}$). $R-A$ is a general term representing all possible attractive and
128 repulsive stresses between clay particles.

129
130 By examining the effective stress in a stiff indurated clay rock theoretically and experimentally,
131 Zhang (2017) concluded that in a dense clay-water system, the effective stress is transferred

132 through the solid-solid contact between non-clay mineral grains and for the most part, the bound
 133 pore water in narrow pores, i.e.:

$$134 \quad \sigma' = \sigma_s + \sigma_l \quad (5)$$

135 where σ_l represents the average net repulsive force acting on the bound water-film area divided
 136 by the total cross-sectional area ($\text{ML}^{-1}\text{T}^{-2}$). The experimental results of Zhang (2017) suggested
 137 that for stiff indurated clay rock, the swelling pressure is almost equal to the effective stress.
 138 Mašín and Khalili (2015) referred the net electrical stress acting on water-films between clay
 139 particles as σ^{R-A} and argued that this kind of stress mainly controls the mechanical behaviour of
 140 soils with prevailing face-to-face particle arrangement. In this regard, the σ_l and σ^{R-A} refer to the
 141 same kind of stresses acting in the dense clay-water system.

142

143 Therefore, for the low-compressibility zone where the particle arrangement is dominated by the
 144 face-to-face feature, the term $\Delta\sigma_v'$ in Eq. 2 should be revisited. At each loading step the σ^{R-A} is
 145 assumed to be equal to the swelling pressure P_s at the corresponding density. The vertical
 146 effective stress $\sigma_{v,i}'$ at a given step i is determined by subtracting the $P_{s,i}$ value from the applied
 147 vertical stress $\sigma_{v,i}$ based on Eq. 6. Then, a new $m'_{v,i}$ is determined using the modified $\sigma_{v,i}'$ following
 148 Eq. 7. Thus, a modified indirect value k'_{ind} can be further calculated by substituting the new $m'_{v,i}$
 149 in Eq. 1. With such modifications, the new k'_{ind} is expected to be closer to the direct value.

$$150 \quad \sigma'_{v,i} = \sigma_{v,i} - P_{s,i} \quad (6)$$

$$151 \quad m'_{v,i} = \frac{\Delta e_i}{(\sigma'_{v,i} - \sigma'_{v,i-1})(1 + e_{i-1})} \quad (7)$$

152

153 It is worth noting that the modification is proposed by incorporating the physico-chemical
 154 effects into the effective stress equation for dense expansive clays. In other words, the proposed
 155 approach is an extension of Terzaghi's consolidation theory.

156 **Complementary experiment**

157 To evaluate the validity of the proposed modification, an oedometer test was performed on
158 GMZ bentonite slurry. The bentonite, originated from Inner Mongolia, China, is a Na⁺ bentonite
159 with a montmorillonite fraction of 75.4%. The total cation exchange capacity is 77.30 meq/100g
160 with 43.36, 29.14, 12.33 and 2.51 meq/100g for Na, Ca, Mg and K, respectively. The bentonite
161 powder, with particles smaller than 0.2 mm and a solid particles density of 2.66 Mg/m³, has a
162 liquid limit of 276% and a plastic limit of 37%.

163

164 The slurry was prepared by mixing de-aired distilled water with the bentonite powder to reach
165 a water content of 1.5 times its liquid limit. Care was taken to avoid trapping air bubbles inside.
166 After 24 h sealing for water homogenization, the slurry was carefully poured into the oedometer
167 cell with 50 mm inner diameter to the marked height of 30 mm. The oedometer has a steel
168 porous disk and a filter paper previously placed at the base. Afterwards, a saturated filter paper,
169 a steel porous disk and the piston were placed at the top of the specimen in sequence. The slurry
170 was allowed to pre-consolidate under a stress of 0.013 MPa, which corresponds to the piston
171 weight. The positions of the piston during the pre-consolidation were monitored using a
172 cathetometer to determine the void ratio change.

173

174 When the pre-consolidation was completed, the oedometer cell was placed in a high-pressure
175 load frame, which enables a maximum vertical pressure of 50 MPa to be applied on the
176 specimen. More details about this loading system can be found in Ye et al. (2012). Conventional
177 step loading was applied with ultimate load equal to 41.25 MPa.

178

179 The values of the coefficient of consolidation c_v at the last three consolidation steps, where
180 specimen was expected to be in the low-compressibility zone, were estimated using
181 Casagrande's method for indirectly determining the hydraulic conductivity. Constant head

182 permeability tests were also carried out after consolidation completion at these three steps under
183 1 MPa water injection pressure, by using a volume/pressure controller connected to the
184 oedometer cell. In addition, swelling pressure tests using constant-volume method were
185 performed on statically compacted GMZ bentonite specimens with void ratios taken from the
186 compression curve.

187 **Application to existing data**

188 The attempts of introducing a modified effective stress into the indirect method are made on
189 the tested GMZ bentonite slurry, as well as three bentonites in the low-compressibility zone
190 from literatures. Results are summarized in Table 2 and graphically shown in Fig. 4. It is worth
191 noting that the values of swelling pressure P_s of GMZ bentonite were deduced from the swelling
192 pressure-dry density relationship determined by Ye et al. (2007), while those for Kunigel and
193 Fourges bentonites were deduced from the correlations established by Wang et al. (2012) based
194 on the literature data. All these swelling pressure-dry density expressions are given in Table 2.
195 As expected, since the external stress is partially supported by the physico-chemical forces
196 between inter-particles, the modified compressibility coefficient m'_v increases as less
197 incremental stress is required to cause a certain decrease in void ratio in each loading step
198 according to Eqs. 6 and 7. In other words, from the perspective of permeability, as compared
199 to the circumstance before modification, it is easier for the specimen in loading step i to drain
200 water with volume change of Δe_i since less incremental effective stress is needed. Therefore,
201 the modified indirect value k'_{ind} increases and becomes much closer to the direct value k_d , making
202 a significant decrease of k_d/k'_{ind} ratio. This, in turn, supports the idea of $\sigma^{R-A} = P_s$ in the case of
203 compression of orientated face-to-face particles. Note that parameter c_v is determined based on
204 the settlement-time curves at each loading step using the common Casagrande method. As
205 negligible free water is expected to be involved in the low-compressibility zone, the
206 consolidation process must mainly depend on adsorbed water, thus physically much more
207 complicated. However, as the void ratio changes a little in this zone, the values of c_v should

208 change a little too. This is evidenced by the similar c_v values at different stresses for a given
209 soil in Table 2. Further examination shows that the improvement of k_d/k_{ind} results of GMZ
210 bentonite, range from 1.2 to 1.9, is more significant than that of other soils ranging from 1.7 to
211 3.8 (Table 2). It is normally due the different accuracies of obtaining swelling pressures: tested
212 on compacted specimens for GMZ bentonite slurry, deduced from different expressions by Ye
213 et al. (2007) for compacted GMZ bentonite and Wang et al. (2012) for the rest two slurries.
214 Furthermore, it is important to note that the swelling pressures used for the three slurries are
215 determined/estimated from the experiments on compacted soils. As for GMZ bentonite, better
216 improvement in k_d/k_{ind} is found in the compacted specimens than the slurry ones (see also Table
217 2), indicating the idea that in highly compacted bentonite, the net stress σ^{R-A} acting on water-
218 films between clay particles is equal to its swelling pressure, also, the necessity of determining
219 the σ^{R-A} in slurry at different void ratios. Better results of k_d/k_{ind} are expected when the σ^{R-A} is
220 obtained with the soils tested in slurry state.

221

222 **Conclusions**

223 The data of hydraulic conductivity k of undisturbed, remoulded and compacted expansive soils,
224 determined in the laboratory by direct and indirect methods are collected and compared,
225 showing that in the primary compression zone which is characterised by a high compressibility
226 the two methods give similar results, while in the low-compressibility zone the indirect method
227 gives much lower hydraulic conductivity.

228

229 In the low-compressibility zone, c_v is found to be almost constant and the difference between
230 the direct and indirect methods is attributed to the effect of physic-chemical interaction. The
231 results of the first attempt with consideration of a modified effective stress accounting for such
232 interaction show that much closer hydraulic conductivity can be obtained between the direct
233 and indirect methods, showing the relevance of such an approach.

234

235 It is worth noting that while directly measuring the hydraulic conductivity (k_d), there must be a
236 certain range of error in the test results even though the test is carried out by strictly following
237 the testing standards. However, as the data obtained here are quite rich, showing the same
238 variation trend, it is believed that this kind of test error does not affect the general conclusion
239 drawn in this paper. More data about more expansive clays are of course needed to further
240 verify this approach.

241

242 **Acknowledgements**

243 The authors wish to acknowledge the support of the European Commission by the Marie
244 Skłodowska-Curie Actions HERCULES - Towards Geohazards Resilient Infrastructure Under
245 Changing Climates (H2020-MSCA-RISE-2017, 778360) and Shanghai Pujiang Talent
246 Program (18PJ1410200).

247

248 **References**

249 ASTM, 1993. D5856: Standard Test Method for Measurement of Hydraulic Conductivity of
250 porous material using a rigid-wall, Compaction-mold Permeameter. ASTM International,
251 West Conshohocken, PA, USA.

252 ASTM, 2010. D5084: Standard test methods for measurement of hydraulic conductivity of
253 saturated porous materials using a flexible wall permeameter. ASTM International, West
254 Conshohocken, PA, USA.

255 ASTM, 2011. D7100: Standard Test Method for Hydraulic Conductivity Compatibility Testing
256 of Soils with Aqueous Solutions. ASTM International, West Conshohocken, PA, USA.

257 Bolt, G.H., 1956. Physico-chemical analysis of the compressibility of pure clays. *Géotechnique*,
258 6(2), 86-93.

259 Casagrande, A., and Fadum, R.E. 1944. Reply to discussions on Application of soil mechanics
260 in designing building foundations. ASCE Transaction Paper, No. 2213, 383-490.

261 Cui, Y.J., Nguyen, X.P., Tang, A.M., Li, X.L. 2013. An insight into the unloading/reloading
262 loops on the compression curve of natural stiff clays. *Applied Clay Science*, 83: 343-348.
263 doi:10.1016/j.clay.2013.08.003.

264 Daniel, D.E. 1994. State-of-the-art: Laboratory hydraulic conductivity tests for saturated soils.
265 Hydraulic conductivity and waste contaminant transport in soil. ASTM STP 1142, David
266 E Daniel and Stephen J Trautwein, Eds., ASTM, Philadelphia.

267 Deng, Y.F., Cui, Y.J., Tang, A.M., Nguyen, X.P., Li, X.L., Greet, M.V. 2011. Investigating the
268 pore-water chemistry effects on the volume change behaviour of Boom clay. *Physics and
269 Chemistry of the Earth, Parts A/B/C*, 36(17): 1905-1912. doi:10.1016/j.pce.2011.07.016.

- 270 Lambe, T.W. 1960. A mechanistic picture of shear strength in clay. In Research conference on
271 shear strength of cohesive soils, ASCE, 555-580.
- 272 Malusis, M.A., Barben, E.J. and Evans, J.C. 2009. Hydraulic conductivity and compressibility
273 of soil-bentonite backfill amended with activated carbon. *Journal of geotechnical and*
274 *geoenvironmental engineering*, 135(5): 664-672. doi:10.1061/(ASCE)GT.1943-
275 5606.0000041
- 276 Marcial, D., Delage, P. and Cui, Y.J. 2002. On the high stress compression of bentonites.
277 *Canadian Geotechnical Journal*, 39(4): 812-820. doi: 10.1139/T02-019.
- 278 Mašín, D. and Khalili, N. 2015. Swelling phenomena and effective stress in compacted
279 expansive clays. *Canadian Geotechnical Journal*, 53(1): 134-147. doi:10.1139/cgj-2014-
280 0479.
- 281 Mesri, G. and Olson, R.E. 1971. Mechanisms controlling the permeability of clays. *Clays and*
282 *Clay Minerals*, 19(3): 151-158. doi: 10.1346/CCMN.1971.0190303.
- 283 Mesri G., Feng, T.W., Ali, S., Hayat, T.M. 1994. Permeability characteristics of soft clays.
284 *Proc. of the 13th Int. Conf. on Soil Mechanics and Foundation Engineering*, Vol 2, Japanese
285 *Society of Soil Mechanics and Foundation Engineering*, Tokyo, 187-192.
- 286 Mesri, G. and Funk, J.R. 2015. Settlement of the kansai international airport islands. *Journal of*
287 *Geotechnical and Geoenvironmental Engineering*, 141(2): 04014102.
288 doi:10.1061/(ASCE)gt.1943-5606.0001224.
- 289 Nguyen, X.P., Cui, Y.J., Tang, A.M., Deng, Y.F., Li, X.L., Wouters, L. 2013. Effects of pore
290 water chemical composition on the hydro-mechanical behavior of natural stiff clays.
291 *Engineering Geology*, 166: 52-64. B.V. All rights reserved.
292 doi:10.1016/j.enggeo.2013.08.009
- 293 Pusch, R., Hokmark, H., and Borgesson, L., 1987. Outline of models of water and gas flow
294 through smectite clay buffers. SKB Technical Report 87-10.
- 295 Retnamony, G.R., Robinson, R.G. and Allam, M.M. 1998. Effect of clay mineralogy on
296 coefficient of consolidation. *Clays and clay minerals*, 46(5): 596-600.
297 doi:10.1346/CCMN.1998.0460514
- 298 Sridharan, A. and Nagaraj, H.B. 2004. Coefficient of consolidation and its correlation with
299 index properties of remolded soils. *Geotechnical Testing Journal*, 27(5): 469-474.
- 300 Sridharan, A. and Rao, G.V. 1973. Méchanisms controlling volume change of saturated clays
301 and the role of the efective stress concept. *Géotechnique*, 23(3): 359-382.
302 doi:10.1680/geot.1973.23.3.359
- 303 Terzaghi, K. 1936. The shearing resistance of saturated soils and the angle between the planes
304 of shear. In *International Conference on Soil Mechanics and Foundation Engineering*, pp.
305 54–56. Harvard University Press: Cambridge, MA.
- 306 Taylor, D.W. 1948. *Fundamentals of soils mechanics*. John Wiley, New York.

- 307 Tavenas, F., Brucy, M., Magnan, J.P., La Rochelle, P., Roy, M. 1979. Analyse critique de la
308 théorie de consolidation unidimensionnelle de Terzaghi. *Revue Française Géotechnique*,
309 (7): 29-43.
- 310 Tavenas, F., Leblond, P., Jean, P., Leroueil, S. 1983. The permeability of natural soft clays. Part
311 I: Methods of laboratory measurement. *Canadian Geotechnical Journal*, 20(4): 629-644.
312 doi:10.1139/t83-072.
- 313 Wang, Q., Tang, A.M., Cui, Y.J., Delage, P., Gatmiri, B. 2012. Experimental study on the
314 swelling behaviour of bentonite/claystone mixture. *Engineering Geology*, 124: 59-66.
315 doi:10.1016/j.enggeo.2011.10.003.
- 316 Watabe, Y., Yamada, K. and Saitoh, K. 2011. Hydraulic conductivity and compressibility of
317 mixtures of Nagoya clay with sand or bentonite. *Géotechnique*, 61(3): 211-219.
318 doi:10.1680/geot.8.P.087
- 319 Ye, W.M., Schanz, T., Qian, L.X., Wang, J., Arifin 2007. Characteristics of swelling pressure of
320 densely compacted Gao-Mao-Zi bentonite GMZ01. *Chinese Journal of Rock and
321 Mechanics and Engineering*, 26(2): 3861-3865.
- 322 Ye, W.M., Zhang, Y.W., Chen, B., Chen, Y.G., Zheng, Z.J., Cui, Y.J. 2012. Investigation on
323 compression behaviour of highly compacted gmz01 bentonite with suction and
324 temperature control. *Nuclear Engineering & Design*, 252: 11-18. doi:
325 10.1016/j.nucengdes.2012.06.037.
- 326 Ye, W.M., Zhang, F., Chen, B., Chen, Y.G., Wang, Q., Cui, Y.J. 2014. Effects of salt solutions
327 on the hydro-mechanical behavior of compacted GMZ01 Bentonite. *Environmental earth
328 sciences*, 72(7): 2621-2630. doi:10.1007/s12665-014-3169-x.
- 329 Zhang, C.L. 2017. Examination of effective stress in clay rock. *Journal of Rock Mechanics and
330 Geotechnical Engineering*, 9(3): 479-489. doi:10.1016/j.jrmge.2016.07.008.
- 331 Zhu, C.M., Ye, W.M., Chen, B., Chen, Y.G., Cui, Y.J. 2013. Influence of salt solutions on the
332 swelling pressure and hydraulic conductivity of compacted GMZ01 bentonite.
333 *Engineering Geology*, 166: 74-80. doi: 10.1016/j.enggeo.2013.09.001.

334 **List of Tables**

335 Table 1. Main information of consolidation-permeability tests from the literature

336 Table 2. Information of indirect k before and after modification

337 **List of Figures**

338 Figure 1. Evolution of k_d/k_{ind} during consolidation, together with the compression curves; (a)
339 slurry in the loading range from 1-2000 kPa, (b) slurry in the loading range from 0.001-100
340 MPa, (c) compacted and undisturbed clays in the loading range from 0.01-100 MPa

341 Figure 2. Evolution of c_v during consolidation of three bentonites, together with the
342 compression curves; (a) compacted GMZ bentonite, (b) Kunigel bentonite slurry and Fourges
343 slurry

344 Figure 3. Evolution of m_v together with the compression curves; (a) compacted GMZ bentonite,
345 (b) Kunigel bentonite slurry and Fourges slurry

346 Figure 4. Comparisons of k_{ind} and modified k'_{ind} , together with the compression curves; (a) GMZ
347 bentonite, (b) Kunigel bentonite slurry and Fourges slurry

348

349 Table 1. Main information of consolidation-permeability tests from the literature

<i>Type</i>	<i>Soil</i>	<i>w_L</i>	<i>Loading range</i>	<i>c_v determination method</i>	<i>Permeability test</i>	<i>Reference</i>
Slurry	Kunigel bentonite	474%	0.13-30 MPa	Casagrande's	constant-head	Marcial et al. (2002)
	Fourges clay	112%				
	Carbon-amended bentonite-sand	27%-42%	24-1532 kPa	Casagrande's	falling-head	Malusis et al. (2009)
	Nagoya clay-sand	/	9.8-1256 kPa	Taylor's	falling-head	Watabe et al. (2011)
	Nagoya clay-bentonite	/				
Undisturbed soil	Boom clay	67.2%	0.05-3.2 MPa	Casagrande's	constant-head	Deng et al. (2010)
	Boom clay	67.2%	0.05-3.2 MPa	Casagrande's	constant-head	Ngyuen et al. (2013)
Compacted soil	GMZ bentonite	276%	0.5-42 MPa	Casagrande's	constant-head	Zhu et al. (2013)
						Ye et al. (2014)

350

351 Table 2. Information of indirect k before and after modification

Soil	e	σ_v' (MPa)	P_s (MPa)	Modified σ_v' (MPa)	c_v (m ² /s)	m_v (kPa ⁻¹)	m_v' (kPa ⁻¹)	k_d (m/s)	k_{ind} (m/s)	k_{ind}' (m/s)	k_d / k_{ind}	k_d / k_{ind}'	Data resource
GMZ	0.64	11.57	3.67	7.90	/	/	/	/	/	/	/	/	
bentonite	0.52	17.32	7.12	10.20	7.1×10 ⁻¹⁰	1.2×10 ⁻⁵	3.0×10 ⁻⁵	2.4×10 ⁻¹³	8.4×10 ⁻¹⁴	2.1×10 ⁻¹³	2.9	1.2	this work
slurry	0.46	29.29	14.90	14.39	9.7×10 ⁻¹⁰	3.3×10 ⁻⁶	9.5×10 ⁻⁶	1.2×10 ⁻¹³	3.2×10 ⁻¹⁴	9.3×10 ⁻¹⁴	3.6	1.3	
	0.42	41.25	22.75	18.50	6.5×10 ⁻¹⁰	3.9×10 ⁻⁶	7.6×10 ⁻⁶	9.2×10 ⁻¹⁴	2.6×10 ⁻¹⁴	4.9×10 ⁻¹⁴	3.6	1.9	
Compacted	0.74	5.21	1.66	3.55	1.6×10 ⁻⁹	1.8×10 ⁻⁵	2.5×10 ⁻⁵	5.8×10 ⁻¹³	3.0×10 ⁻¹³	4.8×10 ⁻¹³	2.0	1.2	Zhu et al (2013)
GMZ	0.54	20.98	7.49	13.49	1.2×10 ⁻⁹	5.9×10 ⁻⁶	9.8×10 ⁻⁶	2.1×10 ⁻¹³	8.3×10 ⁻¹⁴	1.4×10 ⁻¹³	2.5	1.5	Ye et al (2014)
bentonite	0.47	38.42	13.39	25.03	1.6×10 ⁻⁹	2.5×10 ⁻⁶	3.8×10 ⁻⁶	1.1×10 ⁻¹³	4.8×10 ⁻¹⁴	7.2×10 ⁻¹⁴	2.3	1.5	
Kunigel	0.47	8.38	2.03	6.35	6.7×10 ⁻¹¹	1.4×10 ⁻⁵	1.7×10 ⁻⁵	3.1×10 ⁻¹⁴	9.7×10 ⁻¹⁵	1.3×10 ⁻¹⁴	3.2	2.3	Marcial et al (2002)
bentonite	0.32	31.23	4.09	27.14	1.0×10 ⁻¹⁰	1.4×10 ⁻⁶	1.5×10 ⁻⁶	6.4×10 ⁻¹⁵	1.5×10 ⁻¹⁵	1.9×10 ⁻¹⁵	4.3	3.4	
Fourges	0.82	8.38	0.59	7.79	4.8×10 ⁻¹⁰	2.0×10 ⁻⁵	2.2×10 ⁻⁵	2.0×10 ⁻¹³	9.8×10 ⁻¹⁴	1.3×10 ⁻¹³	2.5	1.6	
clay	0.74	16.59	1.17	15.42	4.9×10 ⁻¹⁰	5.9×10 ⁻⁶	6.3×10 ⁻⁶	1.4×10 ⁻¹³	2.9×10 ⁻¹⁴	3.8×10 ⁻¹⁴	4.2	3.8	
	0.65	31.23	2.51	28.72	5.3×10 ⁻¹⁰	3.5×10 ⁻⁶	3.8×10 ⁻⁶	4.1×10 ⁻¹⁴	1.9×10 ⁻¹⁴	2.5×10 ⁻¹⁴	2.5	1.7	

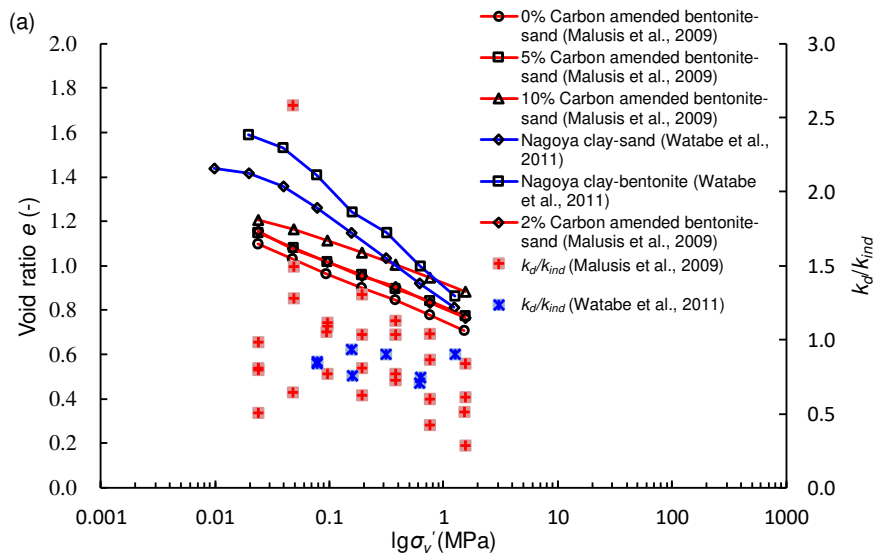
352 * P_s of compacted GMZ bentonite from Ye et al (2014) with distilled water is calculated based on the prediction equation by Ye et al. (2007). $P_s = 1.94 \times 10^{-3} \exp(7.419 \rho_d)$ (MPa), where ρ_d is the dry density

353 of bentonite (Mg/m³).

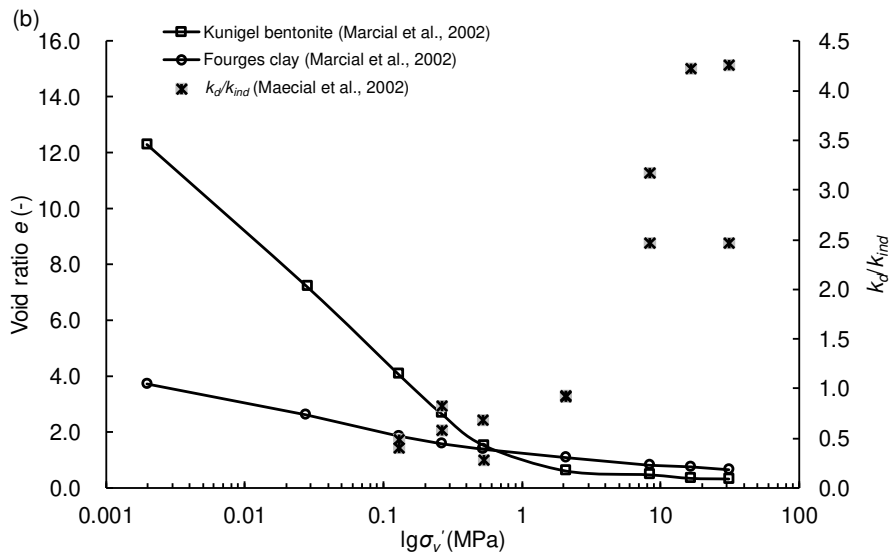
354 P_s of Kunigel and Fourges bentonite are calculated based on the prediction equations by Wang et al. (2012). Kunigel: $P_s = 3.67 \times 10^{-3} \exp(3.32\rho_d)$; Fourges: $P_s = 7.83 \times 10^{-7} \exp(9.24\rho_d)$.

355 ^a data from personal communication

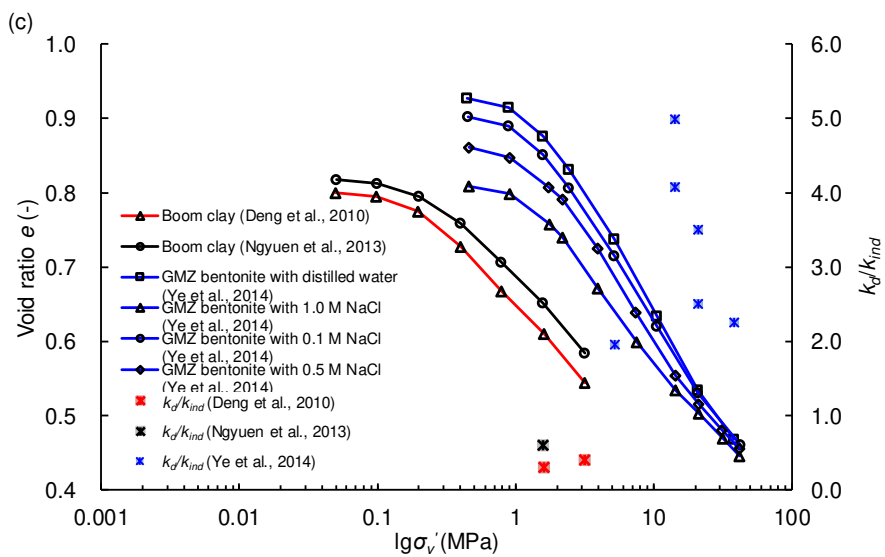
356



357

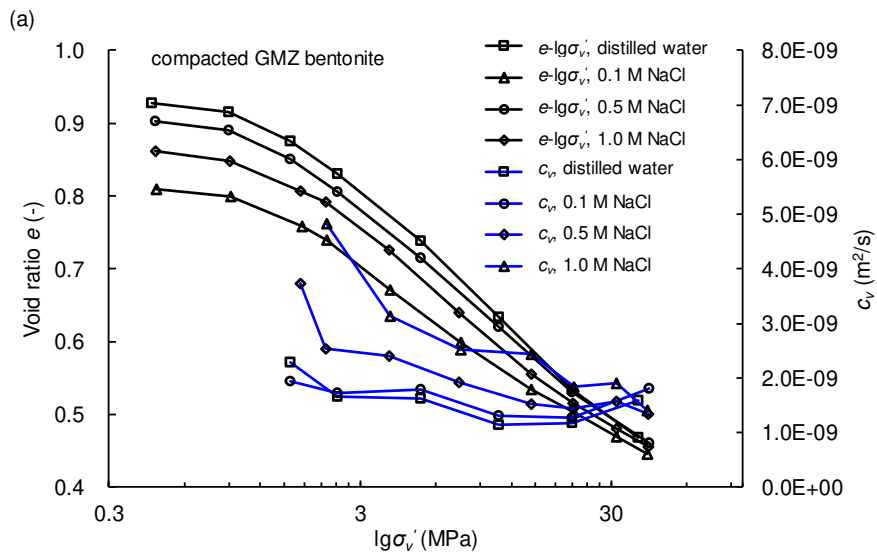


358

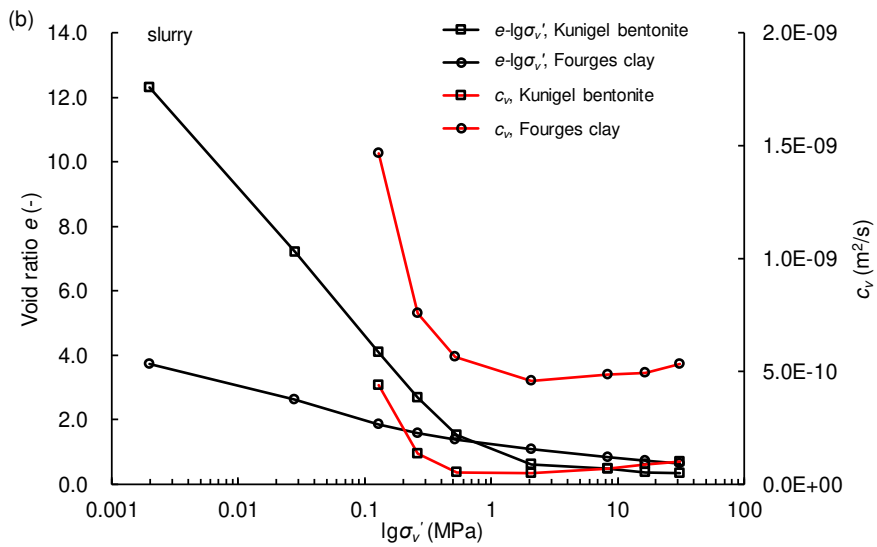


359

360 Figure 1. Evolution of k_d/k_{ind} during consolidation, together with the compression curves; (a)
 361 slurry in the loading range from 1-2000 kPa, (b) slurry in the loading range from 0.001-100
 362 MPa, (c) compacted and undisturbed clays in the loading range from 0.01-100 MPa



363

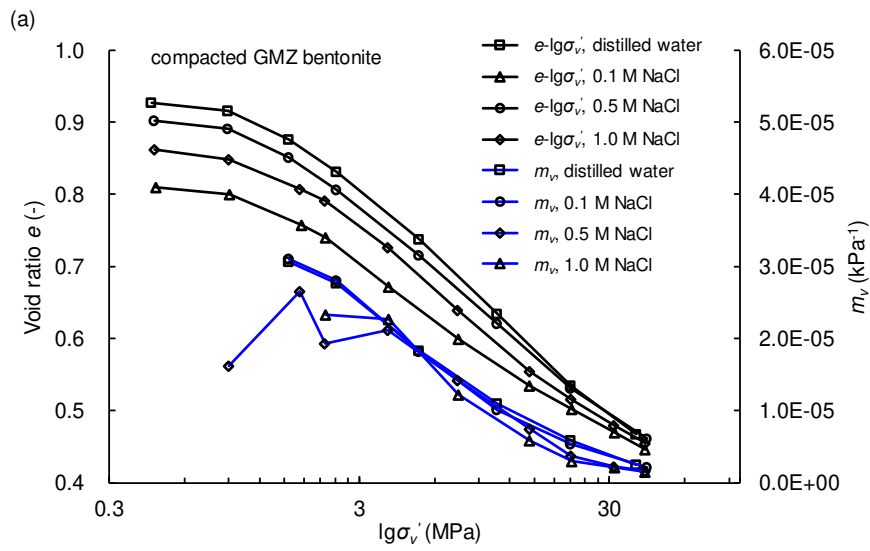


364

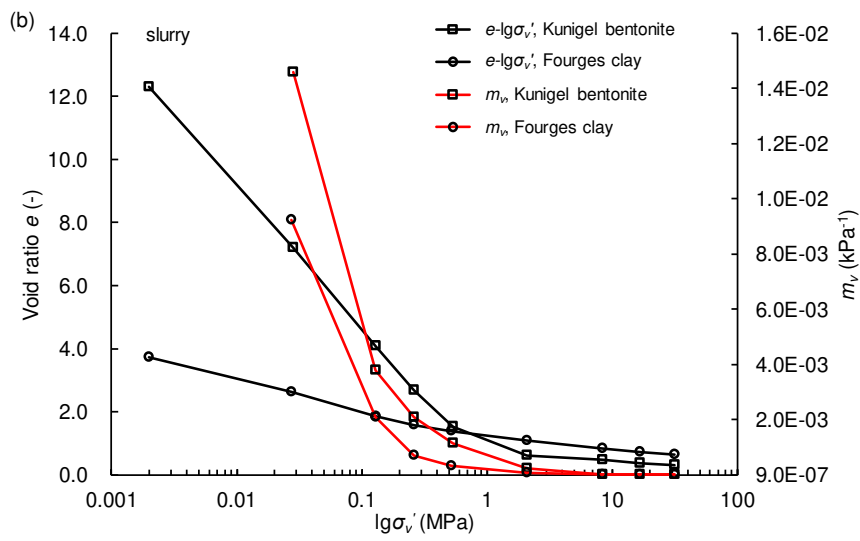
365 Figure 2. Evolution of c_v during consolidation of three bentonites, together with the
 366 compression curves; (a) compacted GMZ bentonite, (b) Kunigel bentonite slurry and Fourges
 367 slurry

368

369



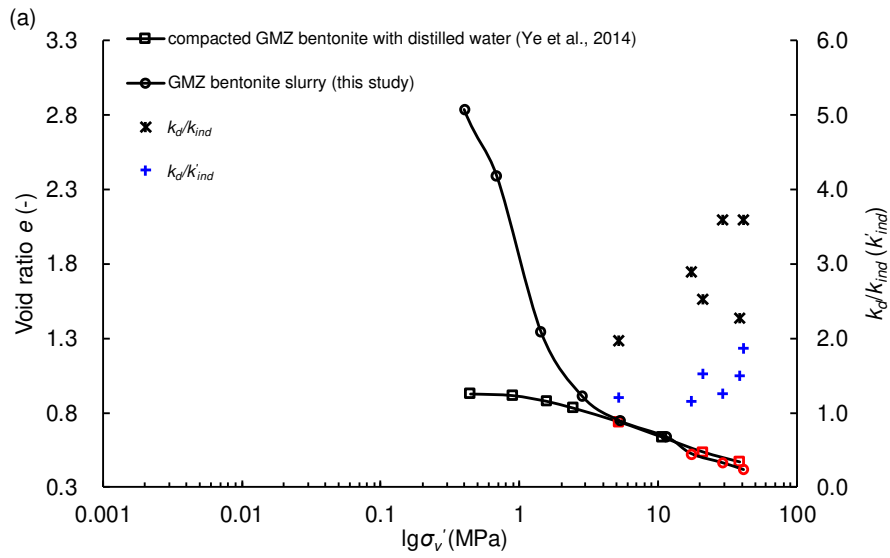
370



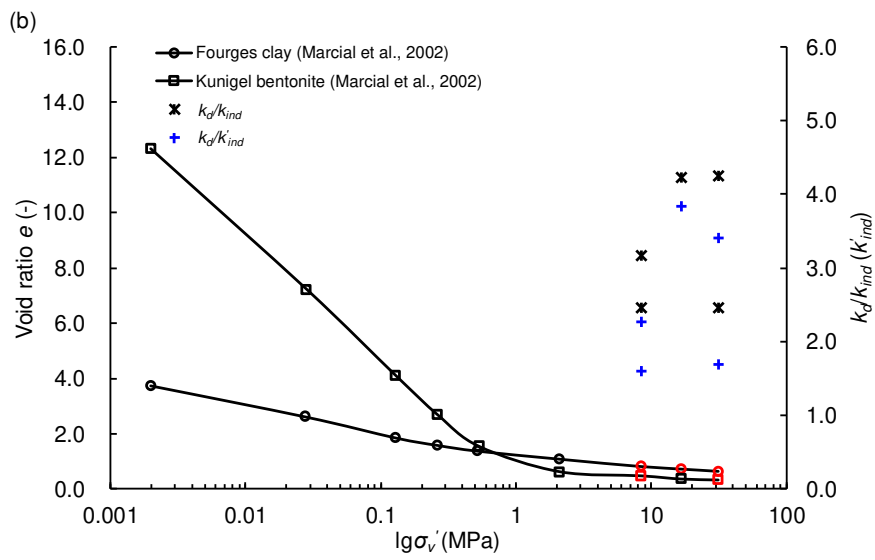
371

372 Figure 3. Evolution of m_v together with the compression curves; (a) compacted GMZ bentonite,

373 (b) Kunigel bentonite slurry and Fourges slurry



374



375

376 Figure 4. Comparisons of k_{ind} and modified k'_{ind} , together with the compression curves; (a) GMZ

377 bentonite, (b) Kunigel bentonite slurry and Fourges slurry